GEM TN-93-264

P_T-Trigger in the End-Cap Muon System: Radial vs. Rectangular Chamber Layouts

A. Korytov
Massachusetts Institute of Technology

January 5, 1993

Abstract:

Shown is the importance of information about theta-angle in end-cap region for muon P_T-trigger. Radial strips and straight strips/tubes are relatively compared.

Jan 5, 1993
A.Korytov
M.I.T.

P_T-TRIGGER IN THE END-CAP MUON SYSTEM: RADIAL VS. RECTANGULAR CHAMBER LAYOUTS.

Mechanical inconvenience of radial layout for a drift tube design for the End-Cap Muon System gave a motivation to re-examine what should be actually measured in the End-Caps to provide p_T trigger.

For simplicity sake, the calculation are done in assumption of an axial magnetic field. This provides fast analytical estimations and is not too far from a real situation (except a region at small θ-angles in vicinity of the iron field concentrator, where a radial component is of about the same magnitude as axial). The actual field components were calculated by J. Sullivan and could be found elsewhere [1].

Fig.1 shows two views of an end-cap sector with a muon track in it. The value of s is a measure of p_T and could be calculated as follows:

$$s \sim \frac{B \cdot L_3^2}{p_T}, \quad \text{where} \quad L_3 = z_3 \cdot \tan\theta / \cos\varphi. \tag{1}$$

The effect of cosφ can be neglected at trigger level ($\cos 11^\circ = 0.98$). Also, to simplify calculations, tanθ will be further replaced by θ (this is accurate at 2% level for angles smaller than 30°). Given that, one gets for s :

$$s \sim \frac{\theta^2}{p_T}. \tag{2}$$

1. Radial Strips.

In case of radial strips, the measured value is an angle Δφ:

$$\Delta\varphi \sim s / L_2 \sim s / r_2 \sim s / (z_2 \cdot \tan\theta) \sim s / \theta \sim \frac{\theta}{p_T} = A \cdot \frac{\theta}{p_T}. \tag{3}$$

This expression makes it clear that Δφ is not a direct measure of p_T and for a constant p_T Δφ is different for different θ-angles. This obviously results in that Δφ alone can not provide a trigger with a sharp turn-on curve if the chamber has a wide range of θ-angles. In the current design $\theta_{max}/\theta_{min} \sim 2$ within one chamber. If the Δφ-trigger is tuned to be 100% efficient for p_T=20 GeV/c (what means all tracks with $\Delta\varphi < \Delta\varphi_\sigma = A * \theta_{max}/p_{TRIGGER}$ are accepted), the tracks with p_T=10 GeV/c at $\theta = \theta_{min}$ will be also accepted.

Assuming that the particle rate $dN/d\eta$ is flat (for any given p_T), one immediately obtains:

$$\frac{1}{N}\cdot\frac{dN}{d\theta}\sim\frac{Const(p_T)}{\theta} \tag{4}$$

This distribution may be used to estimated the chamber efficiency (tuned for a particular $p_{TRIGGER}$) to accept tracks of lower p_T: the trigger ($\Delta\varphi<\Delta\varphi_o=A\theta_{max}/p_{TRIGGER}$) accepts tracks with lower p_T in the angle range from θ_{min} up to $\theta_{max}*(p_T/p_{TRIGGER})$. The result is:

$$\varepsilon = 1-\frac{\ln(p_{TRIGGER}\ /\ p_T)}{\ln 2}, \quad (\text{valid when } 1 < p_{TRIGGER}\ /\ p_T < 2). \tag{5}$$

2. Straight Strips/Tubes.

In the case of a rectangular chamber with straight strips or drift tubes, the measured difference $dx\sim s$ could be treated as a measure of p_T ($\cos\varphi$ factor is again neglected):

$$dx = A\cdot\frac{\theta^2}{p_T}\ . \tag{6}$$

<u>The dependence on θ is even stronger</u> as compared to radial strips and tracks with a p_T as low as 1/4 of $p_{TRIGGER}$ may be accepted at $\theta=\theta_{min}$ (assuming $\theta_{max}/\theta_{min}\sim 2$).

Again, taking into account angle distribution of particles, one can easily obtain the chamber efficiency as follows:

$$\varepsilon = 1-\frac{1}{2}\cdot\frac{\ln(p_{TRIGGER}\ /\ p_T)}{\ln 2}, \quad (\text{valid when } 1 < p_{TRIGGER}\ /\ p_T < 4) \tag{7}$$

Another important remark should be mentioned: for tracks of infinitely high momentum any tube hit in SL3 is <u>uniquely</u> correlated with a corresponding tube in SL2 (independently of θ and φ) – fig.2. Thus, in this context, $\Delta\varphi$ and dx are equivalent (in case of radial strips, the strip No. in SL2 is the same as the No. of a strip hit in SL3, whilst with straight strips/tubes these numbers are different --- this is the only difference).

3. Drift Tubes with θ information.

The drift tubes have an excellent feature: time difference from both ends of a wire provides information about localization of a track along a wire with an accuracy determined by a TDC bin width only. Fig.3 [2] shows the accuracy achieved in the LSDT's [3] with 1 ns bin width TDC's (LeCroy 2277). Expected sigma of a distribution is 17.3 cm in a good agreement with the measured values (sigma=17.3 cm, RMS=18.2 cm). However, it is not the resolution that is so good about drift tubes. The real merit is that this information is available from the same tubes which give a p_T measurement (trigger). This information is therefore available immediately without any problem of combinatorial combinations (ghosts) which appear in a system with independent measurements of both coordinates. If a radial coordinate along the chamber (r) is measured independently of a coordinate across it and one would like to use r for p_T trigger, then an extraction of θ information would require a pattern recognition in time scale of L1-trigger. This does not seem to be feasible.

On the other hand, in the drift technology this information is easily available and certainly may be used in trigger. Also, I.Pless noted [3] that RPC's can provide correlated measurements of both coordinates (however, confusion could occur if two tracks are separated by less than 1 m).

The expression (6) may be re-written as:

$$p_T = A \cdot \frac{\theta^2}{dx} \quad \text{and} \quad \theta \sim r / z_3 \,, \quad \text{if } r \text{ is calculated in SL 3.} \tag{8}$$

This can be converted into p_T resolution:

$$\frac{\delta p_T}{p_T} = 2\frac{\delta r}{r} \tag{9}$$

where δr ~20cm/sqrt(4) = 10 cm (4 planes in SL3), and r varies from about 4m up to 8 m so that the resolution would also vary along the chamber. It should be noted here, that 10 cm accuracy gives momentum resolution of 5% or better. This essentially means that the momentum resolution (at rigger level) will be determined by strip width and multiple scattering al low momenta, rather than by radial measurements.

4. Summary and discussion.

The trigger turn-on curves for all three possibilities discussed above are presented in fig.4. These curves (expressions (5), (7) and similar function obtained for the expression (9)) are calculations with the only effect taken into account: θ-dependence of the chosen trigger schemes. All other contributions ($\cos\varphi$ dependence, effects of finite strip/tube sizes, multiple scattering in the calorimeter and muon chambers, the realistic B-field) were neglected.

One can see that radial strips are definitely better for trigger purposes when no information along a strip is available.

However, even radial strips apparently have intrinsic insufficiency to provide sharp turn-on trigger.

It is of certain interest, to verify this simple model with a realistic MC made for the case of radial strips by C.Yanagisawa [5] -- fig.5. From a corresponding curve in fig.4 one can conclude that if the trigger is 100% turned on for particular p_T, then it should get 100% turned off for any transverse momentum two times smaller than that chosen p_T (assuming $\theta_{max}/\theta_{min}\sim 2$). A comparison of curves for 10, 20 and 40 GeV/c in fig.5 reveals exactly the same.

Thus, this analytical analysis gives an idea why these curves go this way and not another.

From fig.4. one can see that the availability of information about a hit position along a tube gives significant improvement of the trigger.

Non-zero efficiency at lower p_T can result in dramatic consequences since the p_T-spectrum is very steep. Fig.6 shows an example of p_T-distribution (provided by R.McNeil). For $p_T>3$ GeV/c the spectrum can be reasonably approximated as:

$$\frac{1}{N}\frac{dN}{dp_T} \propto \frac{1}{p_T^{4.15}} \qquad (10)$$

The efficiencies shown in fig.4, being converted with distribution (10), result in p_T-distributions of tracks which would be accepted by the different trigger schemes as shown in fig.7. One can see that a lot of tracks with considerably lower p_T would be accepted if no radial information is used.

Quantitatively, the depth of a 'tail' going towards low momenta in relative units could be define, for example, as follows:

$$\frac{N_{good}}{N_{good}+N_{junk}}, \tag{11}$$

where

$$N_{good}=\int_{1}^{+\infty}\varepsilon(p_T)\cdot\frac{dN}{dp_T}\cdot dp_T \tag{12}$$

$$N_{junk}=\int_{0}^{1}\varepsilon(p_T)\cdot\frac{dN}{dp_T}\cdot dp_T. \tag{13}$$

The following table gives numbers (eq.11) for the trigger schemes discussed above:

Radial Strips (no r information)	27.7%
Straight Strips/Tubes (no r information)	5.6%
Straight Drift Tubes (δr ~10 cm in SL3)	73.7%

One can clearly see the importance of information along strips/tubes.

Acknowledgments.

The fast and simple analysis presented above has appeared as a consiquence of multiple and very fruitful discussions with C.Bromberg, G.Mitselmakher, L.Osborne, L.Rosenson, F.Taylor and many other members of the GEM Muon Group.

References:

1. GEM Magnet TDR.

2. "Performance of a LSDT large scale prototype", to be published.

3. R.Sumner et al., "LSDT's for the GEM Muon System", GEM TN-92-203.

4. I.Pless, Muon Meeting at Tuscon, 3/8/1992.

5. C.Yanagasawa, Muon Meeting at SSC Lab, 4/29/1992.

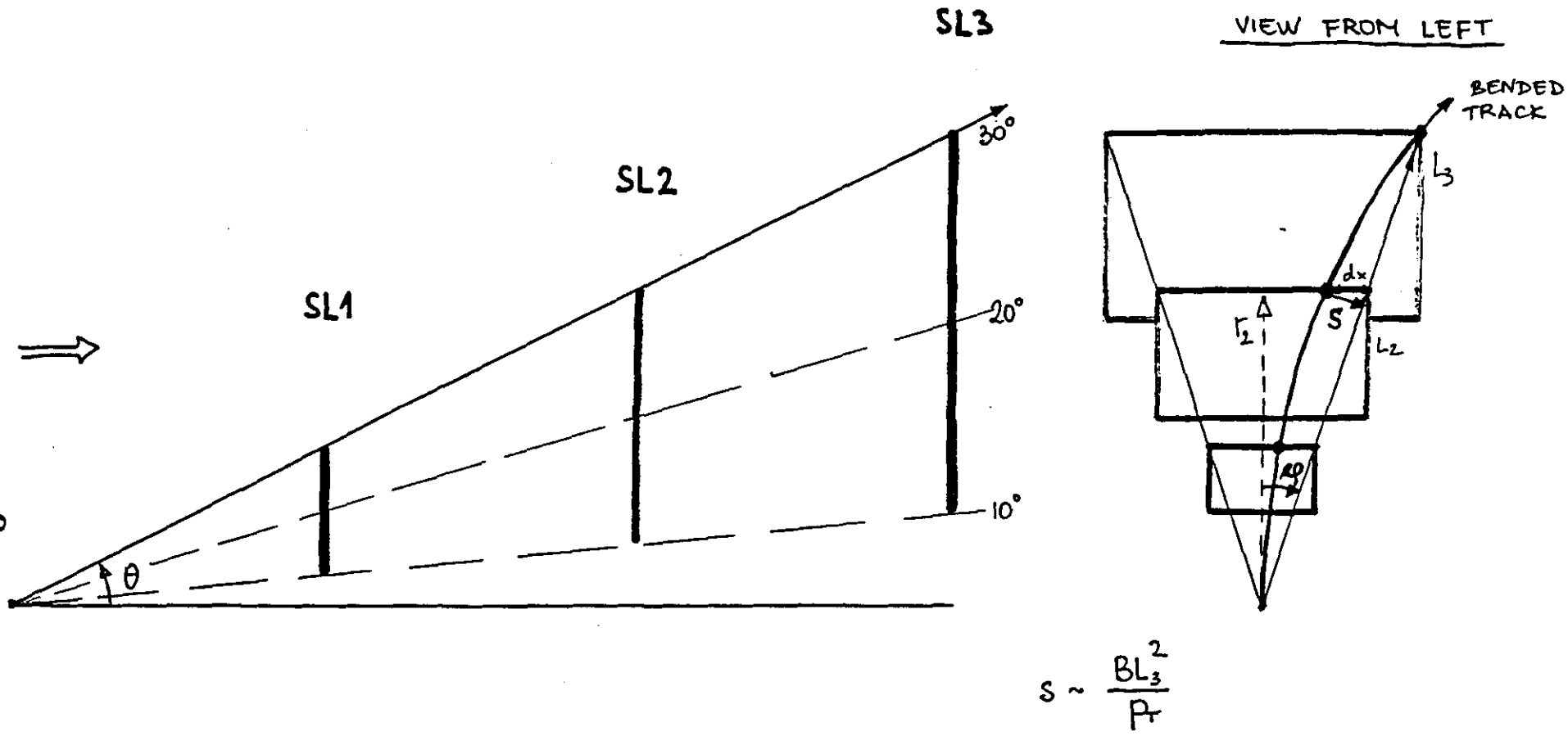

Fig.1. Two views of an end-cap sector with a muon track in it.

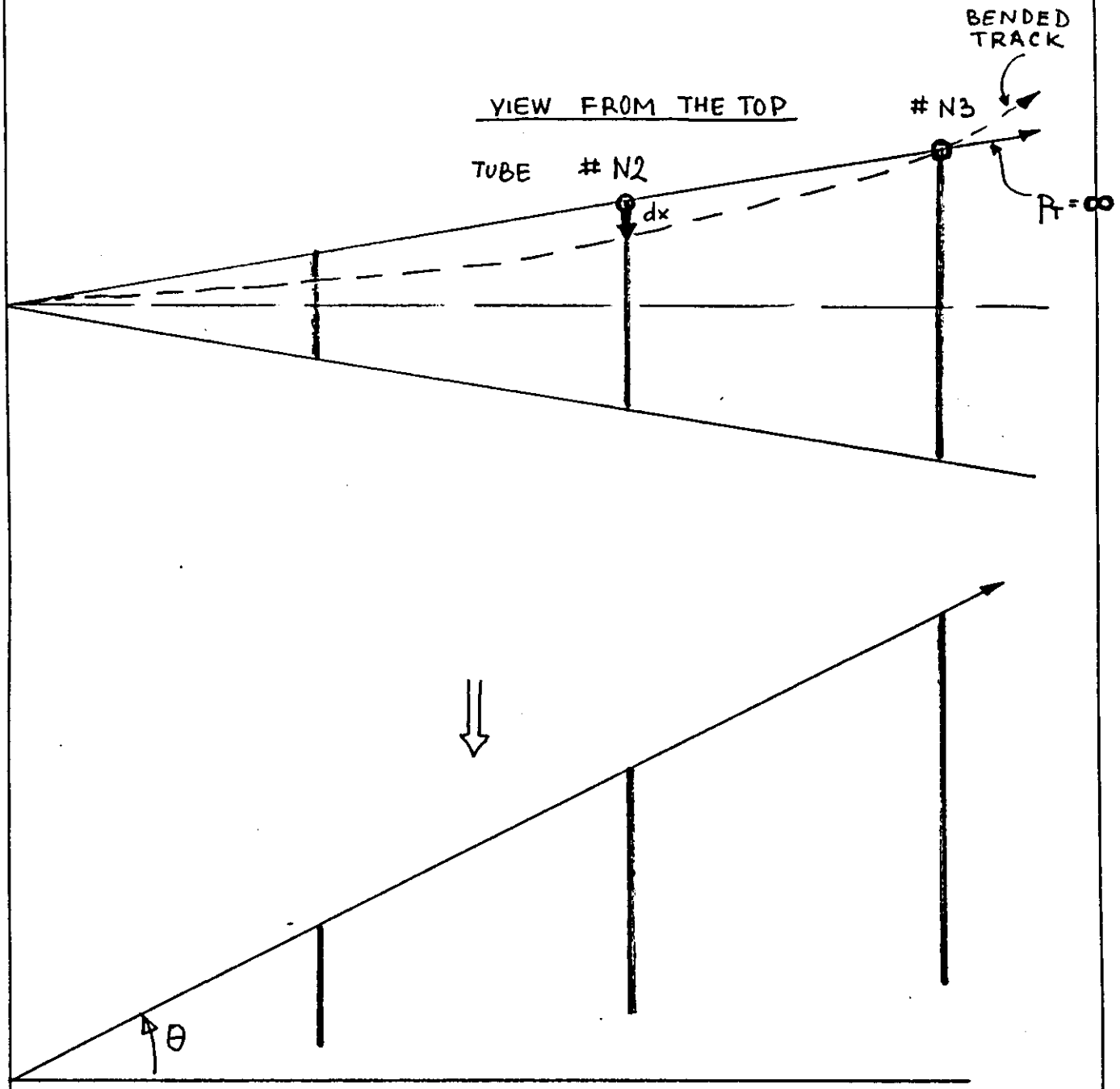

Fig.2. Two views of an end-cap sector with two muon tracks. One of infinitely high momentum looks like a straight line. If this track hits a tube N3 in SL3, no matter where it hits it along the tube it has to hit the tube N2 in SL2. For each N3 there is only one N2.
A deviation dx from N2 is a measure of bending.

PRELIMINARY 9/18/92

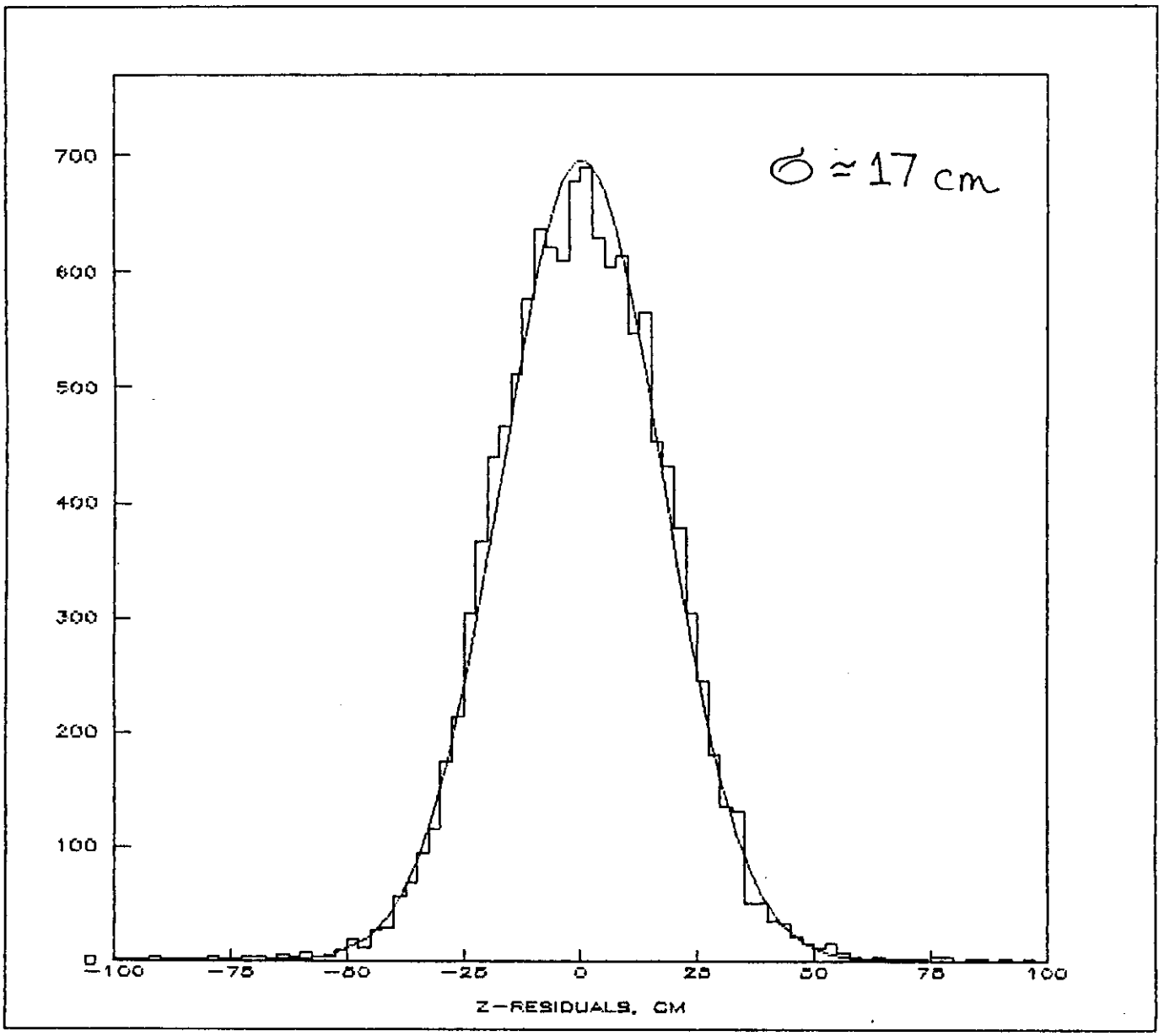

Fig.3. Resolution along a wire in LSDT's as measured by time difference (sigma=17.3 cm, RMS=18.2 cm).

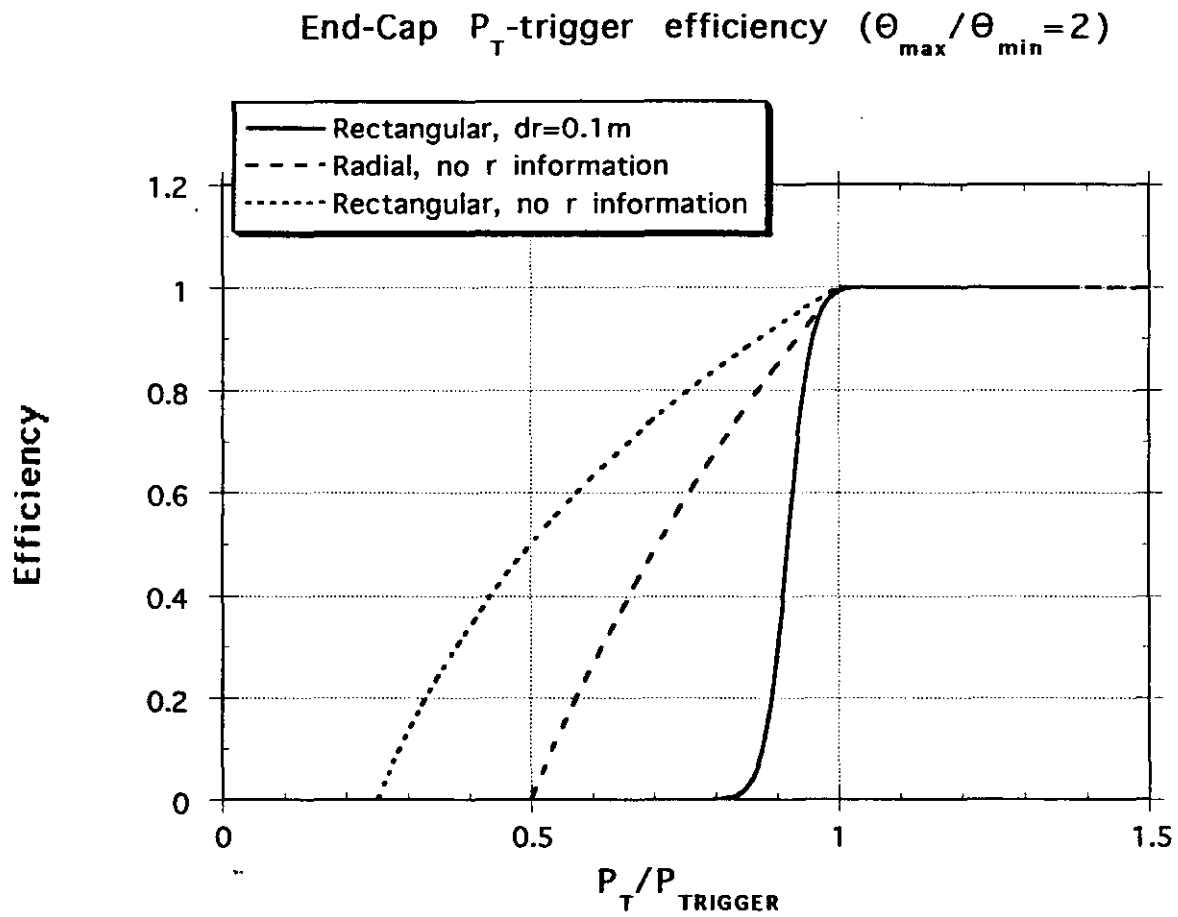

Fig.4. Turn-on curves of a p_T trigger for different chambers (trigger is tuned to have efficiency 99% or higher for $p_T > p_{T0}$).

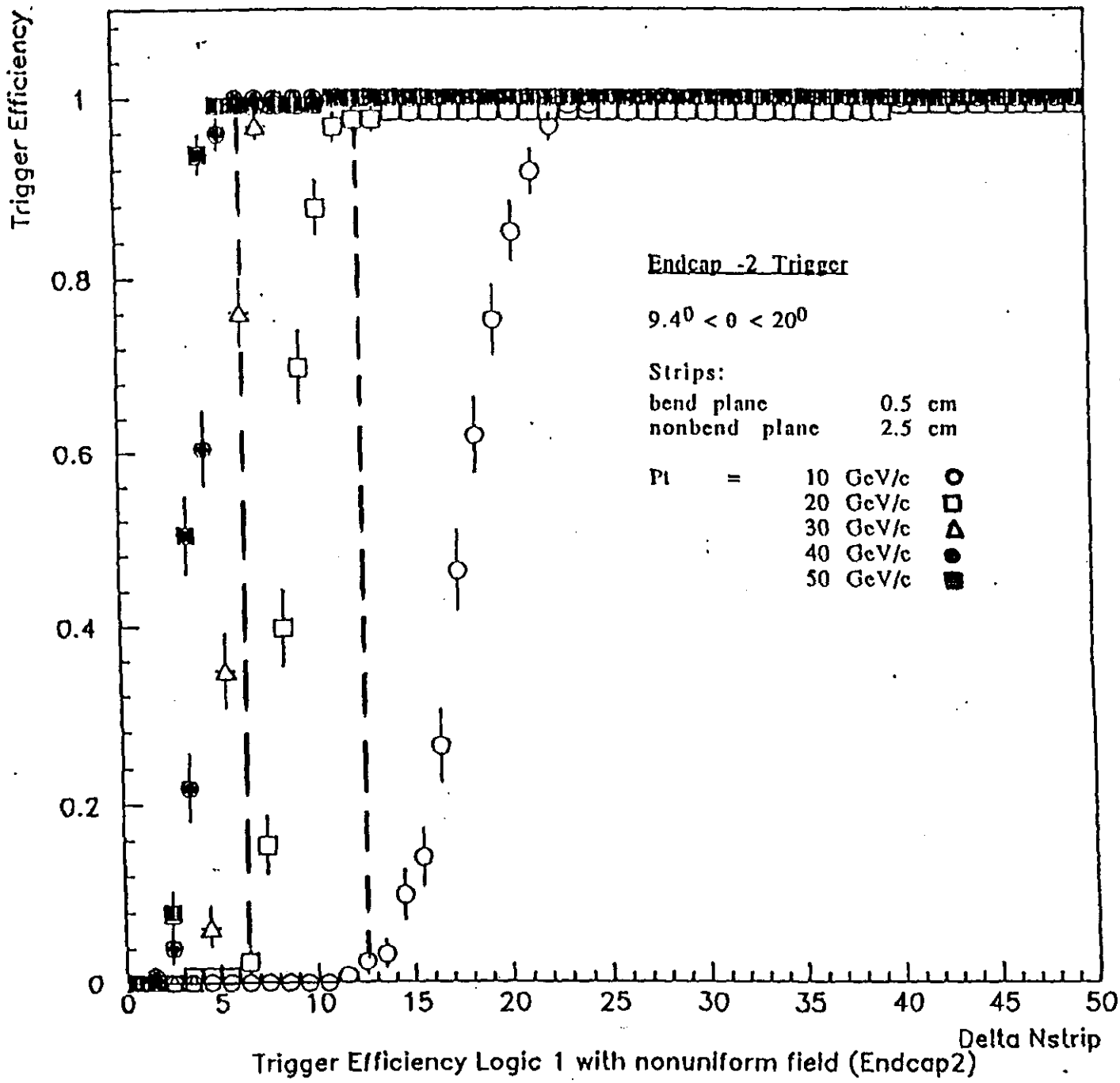

Fig.5. MC Calculations for radial strips. (C.Yanagisawa [5])

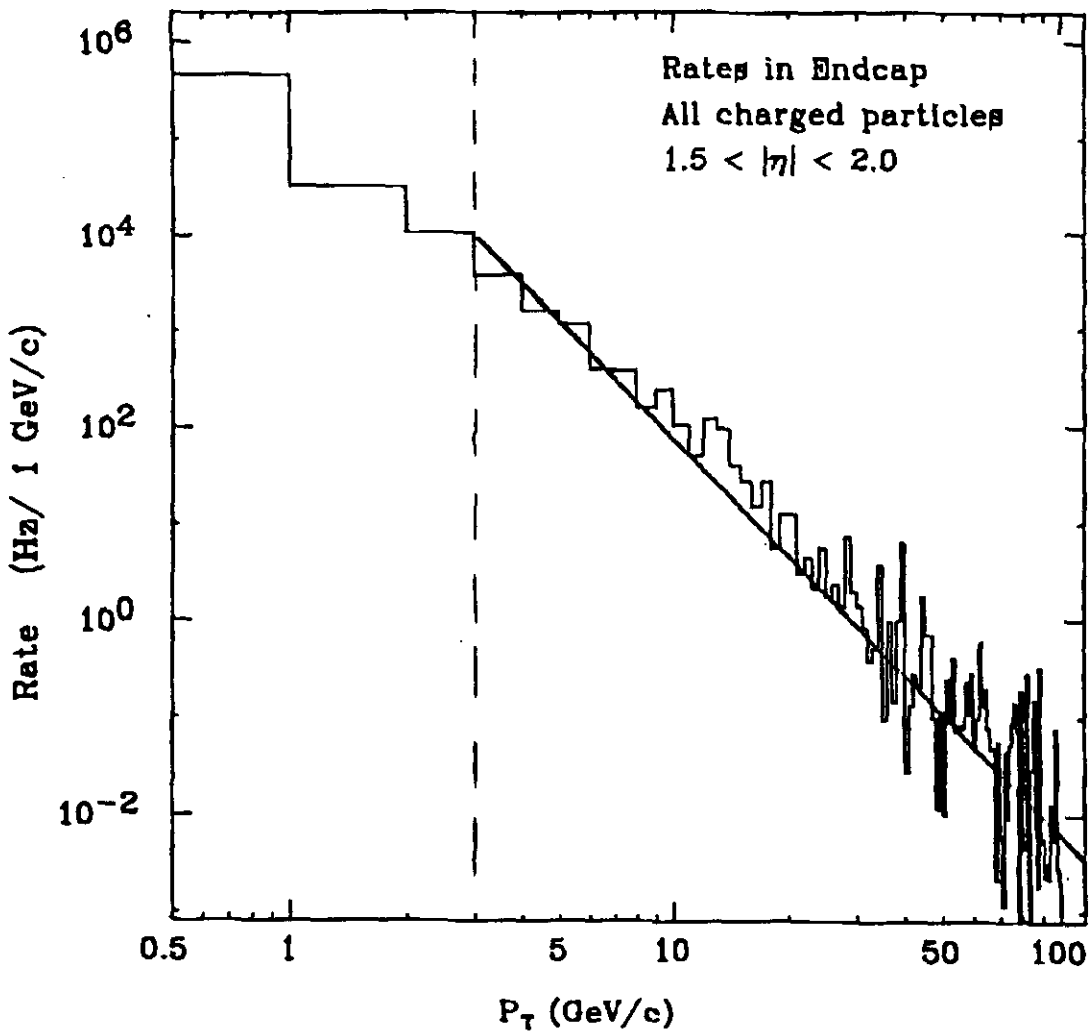

Fig. 6 p_T-Spectrum of particles beyond the calorimeter in the forward region (provided by R. McNeil).

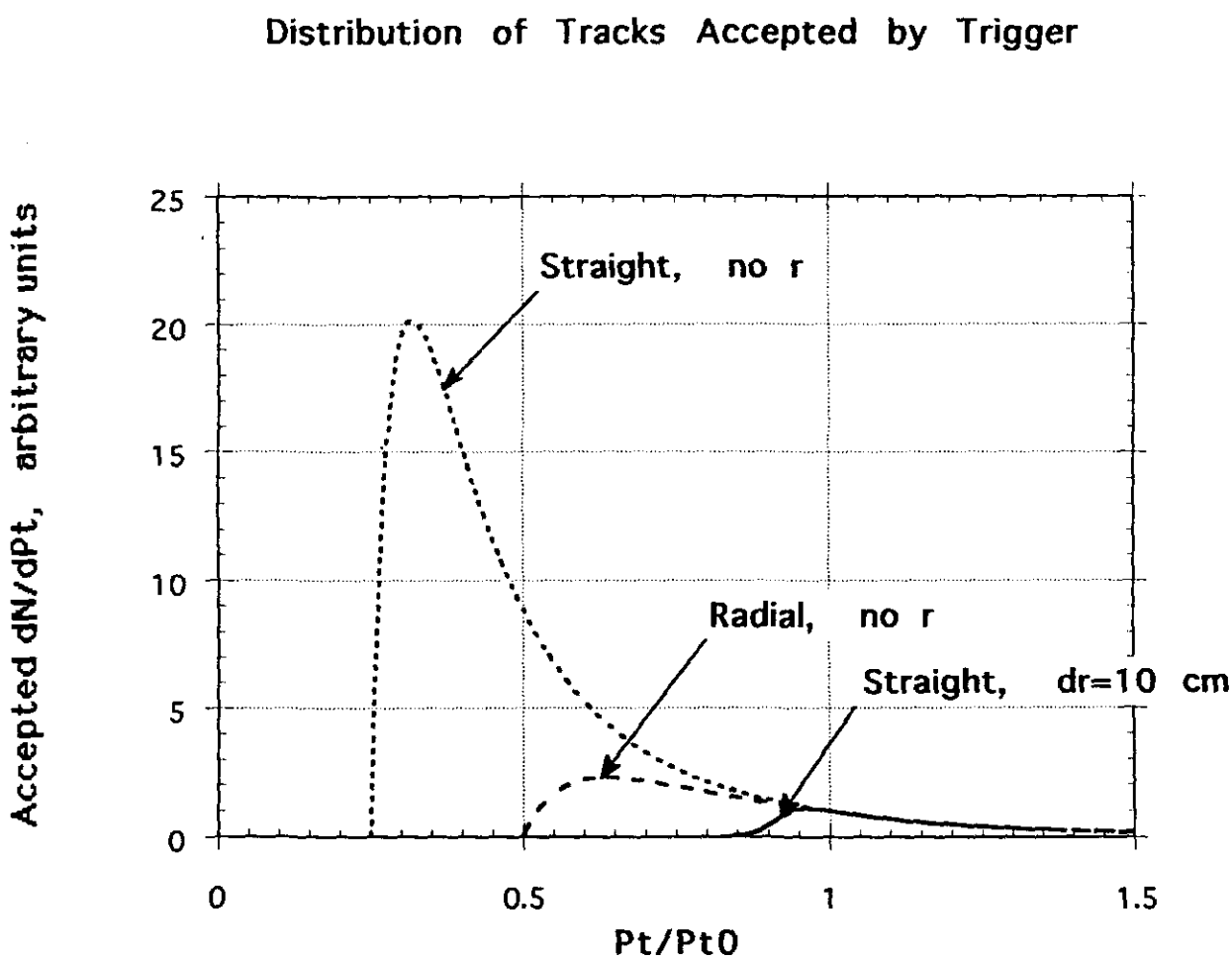

Fig.7. Distribution of tracks accepted by the triggers (tuned to have efficiency 99% or higher for $p_T > p_{T0}$).